JMEPEG (2008) 17:57–63
DOI: 10.1007/s11665-007-9150-z

1059-9495/$19.00

Effect of Electromagnetic Stirring Conditions on Grain Size Characteristic of Wrought Aluminum for Rheo-forging

S.W. Oh, J.W. Bae, and C.G. Kang

(Submitted April 2, 2006; in revised form February 27, 2007)

This article focuses on the microstructural characteristics of A6061 and A7075 wrought Al alloy slurries fabricated by an electromagnetic stirrer (EMS). Billets fabricated by electromagnetic stirrer under different conditions of stirring current, stirring time, and pouring temperatures were investigated for the microstructure and cooling curves of molten alloy which was directly cooled from liquid state to the mushy state during stirring. From the cooling curves and microstructure examination, it is possible to determine the forming time and stirring time required to obtain an optimum structure. Lower pouring temperatures in the range (650–730 °C) led to finer primary-α Al phase grains in both A7075 and A6061 billets. Higher stirring current led to the finer primary-α Al phase. With respect to the effect of stirring time, the primary-α Al phase still appears in dendritic shape for 20 and 40 s of electromagnetic stirring time. The longer electromagnetic stirring time of 60 s led to a finer primary-α Al phase.

Keywords electromagnetic stirring, microstructure, rheology, wrought aluminum

1. Introduction

The car industry around the world has been attempting to integrate all the technological resources capable of developing air pollution-lowering cars. In addition, it has sought to enhance combustion rates according to demand for the improvement of combustion rates and restriction of emissions of combustion gases to eliminate serious environmental contamination in European and advanced countries. As a part of these technologies, semi-solid processing suggested by Flemings in the early 1970s has been attracting a great deal of interest as a technology which boosts the combustion rate and provides lightweight automobiles. This comes at a time when the request from customers regarding high-grad and secure passenger cars has been increasing (Ref 1). The study of the promotion of the combustion rate has been focusing on enhancement of engine efficiency, decrease of air resistance, reduction of tire rolling resistance, and downsizing of car chassis. An alternate way of reducing car weight involves substitution of materials and subsequent development of new forming processes of automobile parts. The idea of reducing car weight in order to elevate the combustion rate has often been proposed in the scientific literature (Ref 2). For example, Sato et al. (Ref 3) produced lower arm parts for automobile by applying rheo-forming, and Kang et al. (Ref 4) demonstrated production of parts by reheating A2024 alloy. In addition, NRC (New Rheo Casting) developed at UBE Inc. in Japan (Ref 5) creates globular microstructures by repeated cooling and heating and Charles (Ref 6, 7) suggested a new electromagnetic rheocaster, which is based on the use of rotating permanent magnets. In spite of these studies, the research to develop casting alloys reached a stage of technological limitation due to low mechanical properties of casting alloys and the geometric complexity of the product. The thixo forming process, in contrast to current casting and forging processes, has not been growing due to the high cost of equipment for reheating and the necessity of the billet to have fine globular microstructures. In order to achieve reductions in manufacturing costs and enhance material properties of the products, fundamental research required to develop forming process superior to current forging and thixo forming processes is a necessity.

In the case of the part-forming process, it is understood that the electromagnetic stirring (EMS) system has been mostly applied to manufacturing of billets of A356 alloy for thixo forming, which is used in continuous casting. Studies regarding rheological forming techniques of structural alloys capable of controlling grain size have not been undertaken.

With rheocasting incorporating the EMS being carried out in the present study, the effect of pouring temperature and stirring current and time on globular microstructures and microstructural change were investigated with regard to the 60 and 70 series aluminum alloys with superior mechanical properties. The EMS technology capable of controlling grain size is suggested as the fundamental forming process which uses the rheological forging process for various structural alloys. The study investigated the relationship between changes in material properties throughout T6 heat treatment and microstructural features.

S.W. Oh and **J.W. Bae**, National Research Laboratory of Thixo/Rheo Forming, Graduate School of Mechanical and Precision Engineering, Pusan National University, Busan 609-735, Korea; and **C.G. Kang**, School of Mechanical Engineering, Pusan National University, Busan 609-735, Korea. Contact e-mail: cgkang@pusan.ac.kr.

2. Manufacturing of Rheological Materials Using EMS

2.1 Electromagnetic Stirring System (EMS)

EMS produces partially solid slurry on solidification. EMS crushes dendritic microstructures occurring during solidification of aluminum melt, where particles crushed by stirring become globular. These globular primary-α Al phase particles are distributed in the melt. EMS reduces shrink defects because solidification time is shorter than that of a fully liquid. This creates a pure dendritic microstructural phase, reduces heat impact on mold when forming the products, and reduces inner pores due to the shorter solidification time. Furthermore, there are advantages, including a reduction in flow defects during mold filling because of the increased viscosity of the semi-solid slurry (Ref 8).

However, in spite of these advantages, the technique has been applied to a limited area composed of billet manufacture by thixo forming and steel production by continuous casting. The present study suggests manufacturing tools of rheological materials such as A6061 and A7075 structural alloys being incorporated into new forming processes by controlling the fraction of solid phase and grain size.

2.2 Design and Fabrication of EMS

Figure 1 depicts a schematic diagram of a horizontal electromagnetic stirring system. To manufacture the electromagnetic stirrer used in this work, the highest priority is the design and manufacture of the core to wind the coil. The core holding the coil which is wound to the core is fabricated to laminate a Si-Zn steel plate, which is 0.35 mm thick. The selection of the inner and outer diameter of the stirrer is of great importance because the dimension of the stirrer is related to the volume of the products; i.e., the inner diameter of the electromagnetic stirrer could be designed to fit the volume of products and the outer diameter to meet the electromagnetic stirring force. The core manufactured in this study, which is capable of producing products 3 kg in weight, has an inner diameter of 140 mm and an outer diameter of 400 mm. Also, this core, which consists of lamination of 400 Si-Zn alloy plates, was fabricated to fix the six phases. The damage of the coil due to heat rapidly generated from the radiation of the melts during stirring is prevented by facilitating the cooling line in the coil. The coil used in the present study consisted of high-conductivity copper which was 1 mm thick, 7 mm height and 7 mm long. The three-phase electricity was applied to the core and cooling water was connected to the inside of the coil. In addition to the connection of the electricity and cooling water, fabrication of the electromagnetic stirrer was completed by interfacing the variable electrical controller capable of controlling the current to the stirrer.

The electromagnetic force of the electromagnetic stirrer was measured by using the Gauss-meter. Figure 2 shows the relation of the applied current with magnetic induction density measured at three different locations of the stirrer; i.e., lower, middle, and upper regions, respectively. The results obtained showed that magnetic flux density is proportional to increases in the applied stirring current. Also, a flux density of 1500 Gauss was measured at the maximum current of 100 A.

2.3 Experiments of EMS and their Results

The EMS used in this experiment was composed of an electromagnetic stirrer, an air cylinder operating the cup upward and downward, a stirring current controller, a furnace capable of melting and holding temperature, and a gas vent. In this study, A7075 and A6061 alloys were used and Table 1 displays the chemical composition of A7075 and A6061. A7075 and A6061 alloys, which were melted down in an electrical resistance furnace, were poured into the electromagnetic stirrer. The parameters of the electromagnetic stirring consisted of stirring current (C), stirring time (t_s), and pouring temperature of melt (T_p). Experimental condition was optimized with adjustable combinations of each experimental

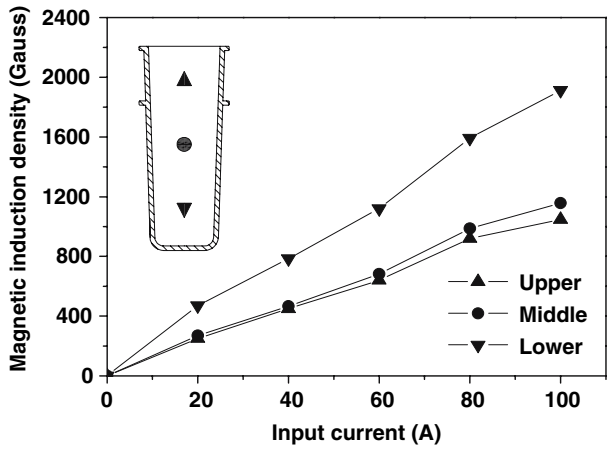

Fig. 2 Measured magnetic flux density

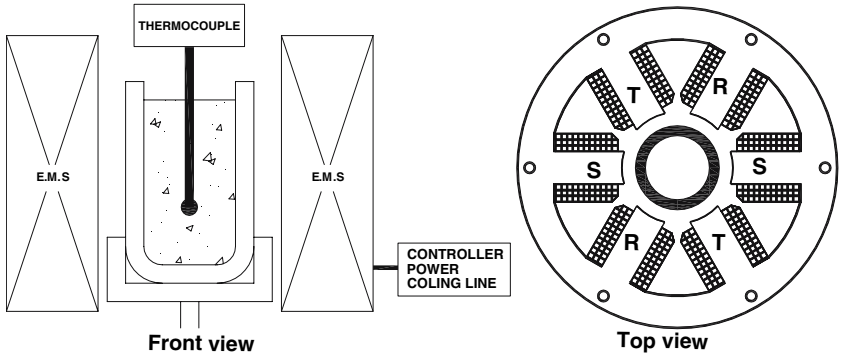

Fig. 1 Schematic diagram of horizontal electromagnetic stirrer

parameter. The microstructural features of billet samples fabricated were studied with analysis of primary-α Al phase particle sizes and their distribution. In addition, we examined their roundness by observing the edge and mid parts in the sample disk taken from the middle of the fabricated billet.

The microstructure was observed after the samples were etched with 35 g of FeCl3 solution-added water (200 mL) and subsequent HNO3, respectively. The microstructural study was performed using optical microscopy and employed the standard polishing technique.

Figure 3 illustrates photographs of microstructures in A7075 alloy observed at axial directions of extruded raw billet and as-cast billet, respectively. These microstructures show that there is no difference between the primary-α Al phase and eutectic phase as well as the phase morphology.

Figure 4 shows the microstructure of an A7075 alloy obtained by electromagnetic stirring at various pouring temperatures; 730, 710, and 670 °C, respectively. And then, a grain size number of the microstructure was measured by planimetic method (ASTM E112) with Lecia MW(Image Analysis Software). When the pouring temperature reached 730 °C, coarse microstructures resulted, whereas fine and globular microstructures were obtained when pouring temperature reached 710 °C. However, when pouring temperature further dropped down to 670 °C, the microstructures continued to coarsen. The values of the grain size numbers were 9.59 at 730 °C, 10.88 at 710 °C, and 7.62 at 670 °C.

Figure 5 shows the observation of the microstructure of A7075 manufactured by EMS under three different stirring currents of 20, 40, and 60 A, respectively. It was observed that the dendritic structure crushed and globularized as the stirring current increased; in particular, at 60 A, a globular structure was obtained. However, it was also observed that above 80 A of stirring current, crushed structures collided with each other and recombined together to yield coarse particles. When stirring current was 80 A, the grain size number was 8.02.

Figure 6 shows the effect of stirring time on the microstructure of A7075 formed by EMS for three different stirring periods of 40, 60, and 90 s, respectively. It was envisioned that the longer the stirring time, the more globular will be the

Table 1 Chemical composition of A6061 and A7075 alloys

	Mg	Zn	Cu	Fe	Si	Mn	Ti	Al
A6061	0.8	...	0.15	0.7	0.4	0.15	0.15	Bal
A7075	2.21	5.53	1.41	0.26	0.1	0.05	...	Bal

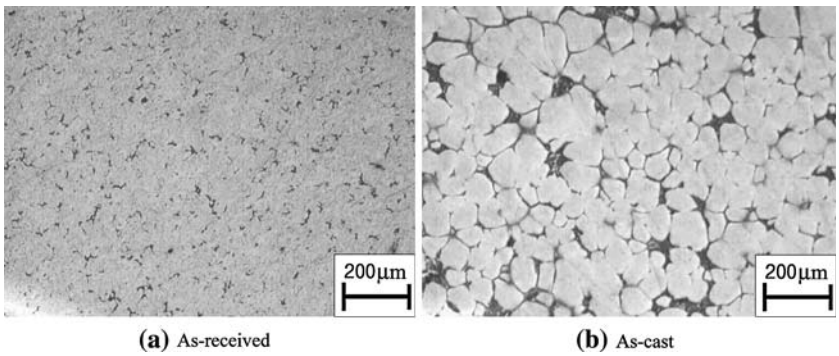

Fig. 3 Microstructures of the as-received and as-cast material in Al7075; (a) As-received, (b) As-cast

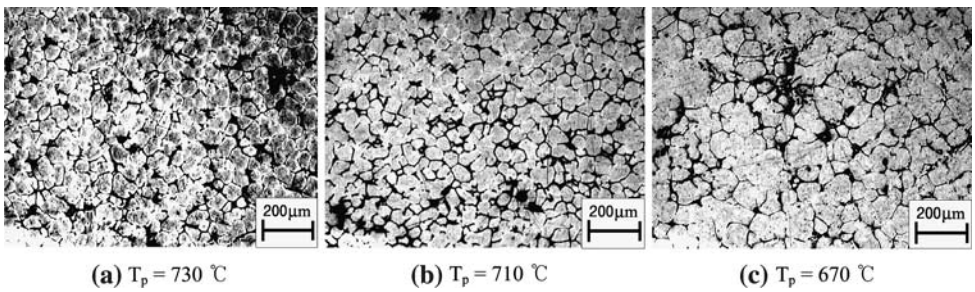

Fig. 4 Microstructures of A7075 alloy obtained by electromagnetic stirrer for variation of pouring temperature (C: 60 A; t_s: 60 s); (a) T_p = 730 °C, (b) T_p = 710 °C, (c) T_p = 670 °C

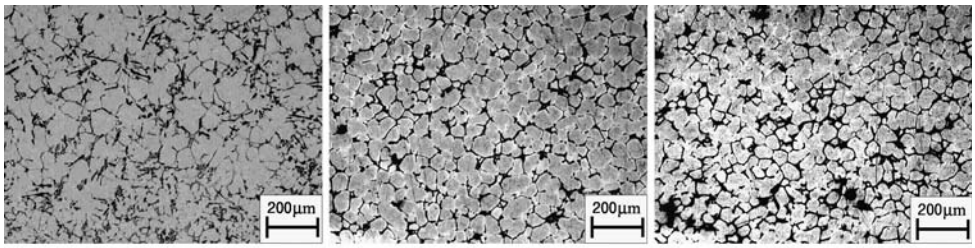

Fig. 5 Microstructures of A7075 alloy obtained by electromagnetic stirrer for variation of stirring current (T_p: 710 °C; t_s: 60 s); (a) C = 20 A, (b) C = 40 A, (c) C = 60 A

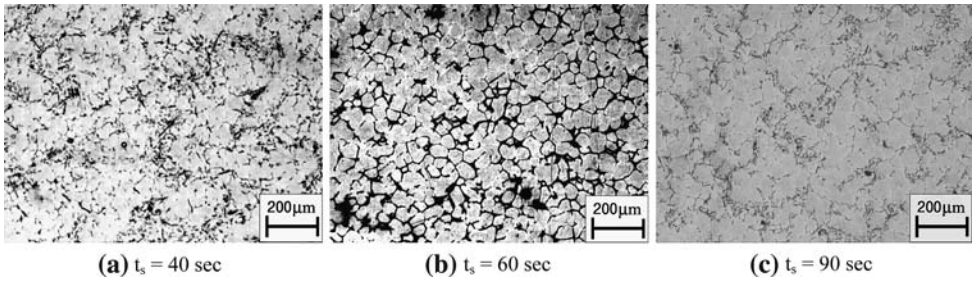

Fig. 6 Microstructures of A7075 alloy obtained by electromagnetic stirrer for variation of stirring time (T_p: 710 °C; C: 60 A); (a) t_s = 40 s, (b) t_s = 60 s, (c) t_s = 90 s

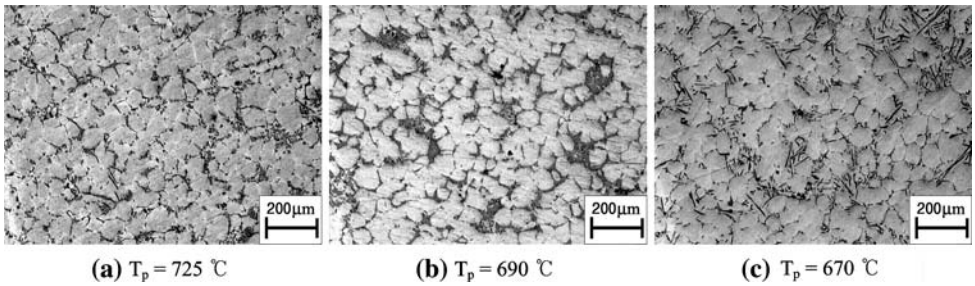

Fig. 7 Microstructures of A6061 alloy obtained by electromagnetic stirrer for variation of pouring temperature (C = 60 A; t_s: 60 s); (a) T_p = 725 °C, (b) T_p = 690 °C, (c) T_p = 670 °C

particles; in particular, 60 s of stirring time resulted in the finest globular structure. However, it was noticed that for more than 60 s of stirring time, crushed structures recombined together and coarsened. The finest globular phase was obtained in A7075 alloy products by EMS at a pouring temperature of 710 °C under the stirring current of 60 A for the stirring time of 60 s.

Figures 7 through 9 show microstructures of A6061 alloys obtained by electromagnetic stirring in terms of variation of pouring temperature, stirring current, and stirring time. Similar to the outcome in A7075 alloys, A6061 products stirred at pouring temperature of 690 °C with 60 A for 60 s, resulted in the finest and most globular phase. On this condition, the grain size number was 9.68.

Figure 10 shows the plots of Vickers hardness of electromagnetic A6061 and A7075 stirred billets according to aging time after solution treatment and subsequent quenching and, Fig. 11 and 12 shows the microstructural changes of A6061 and A7075 alloys as a function of aging time under condition of T6 heat treatment. After-solution treatment of A7075 alloys at 480 °C for 17 h (Ref 9) and measuring the hardness as a function of aging time, the hardness increases as the aging time increases, and the highest hardness of 165 HV under 24 h aging time was obtained. However, the hardness tends to reduce for more than 24 h solution treatment. This could be explained by the fact that since the $MgZn_2$ phase over-precipitates during treatment as aging time increases, the hardness reduces. As was the case with A7075 alloys, after-solution treatment of A6061 alloys at 530 °C for 2 h, the hardness increases as the aging time increases, and the highest hardness of 175 HV under 4 h aging time was obtained (Ref 9, 10). It was noticed that the hardness reduces because Mg_2Si phase over-precipitates during solution treatment as aging time increases.

3. Discussion

To explain the character of wrought A7075, the experimental results of A356 casting alloy fabricated by EMS were

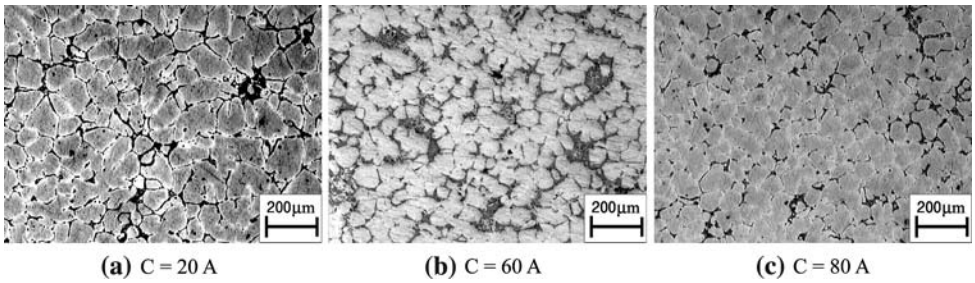

Fig. 8 Microstructures of A6061 alloy obtained by electromagnetic stirrer for variation of stirring current (T_p: 690 °C; t_s: 60 s); (a) C = 20 A, (b) C = 60 A, (c) C = 80 A

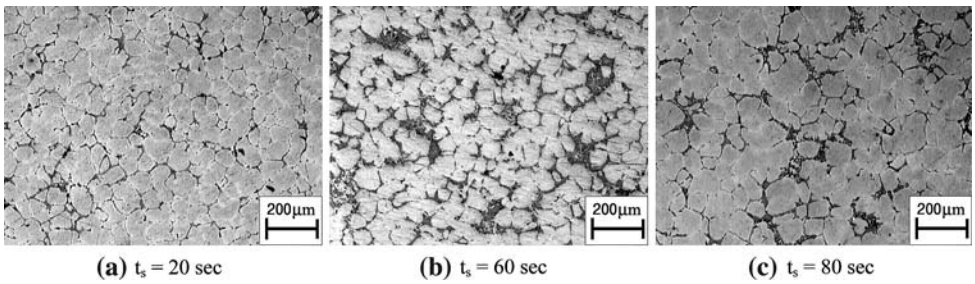

Fig. 9 Microstructures of A6061 alloy obtained by electromagnetic stirrer for variation of stirring time (T_p: 690 °C; C: 60 A); (a) t_s = 20 s, (b) t_s = 60 s, (c) t_s = 80 s

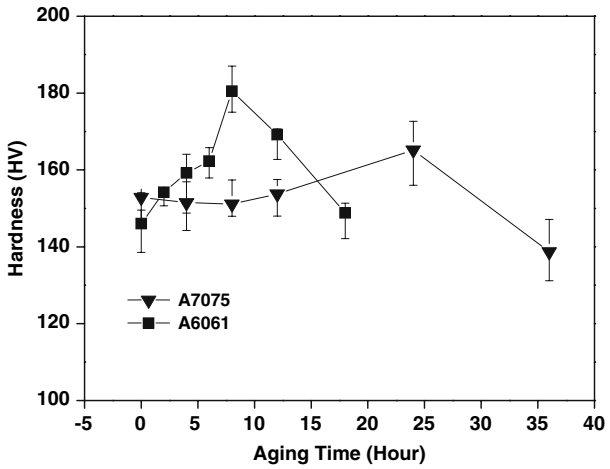

Fig. 10 Hardness for A7075 and A6061 according to aging time after solution treatment (C: 40 A; t_s: 5 s)

compared with that of the A7075. Figure 13 compares microstructures fabricated by EMS in A356 casting alloys and A7075 structural alloys. In the case of casting alloy A356, it is clear that the primary-α Al phase is uniformly distributed in the eutectic phase. Also, the ratio of the eutectic phase to the primary-α Al phase is 50% and distinguishable globules have begun to appear. In contrast, in the case of casting alloy A7075, the eutectic phase takes place less frequently and globules began to appear less frequently than for the casting alloy A356. These results may be caused by temperature differences at a range between 40% and 60% of solid fraction for the casting alloy A356 of 30 °C, or when temperature differences in structural alloy A7075 is about 15 °C. In this state, electromagnetic stirring was not sufficiently transferred to a narrow liquid-solid zone; thus, dendritic phase microstructures had already grown before the dendritic structures crushed due to the electromagnetic stirring force (Ref 11).

Figure 14 illustrates the measurement of the solidification speed for the molten metal during electromagnetic stirring. The melt temperature decreased as the stirring time increased, and solidification of the melts rapidly took place in the melt according to increasing of EMS current. The increase of EMS current generated increasing centrifugal force and rotator force. By centrifugal force, the melt soars at the inner surface of cup, and caves in center of cup. These phenomena cause an increase of the contact-surface of the melt with air, and the temperature falls rapidly.

4. Conclusions

The following conclusions were obtained on A6061 and A7075 structural alloys by EMS:

(1) Fine and globular structure were obtained when the pouring temperature for an A7075 alloy was 710 °C and when pouring temperature for an A6061 alloy was 690 °C.
(2) The dendritic microstructure finely crushed at 60 A of stirring current for both A 7075 and A6061 alloys. However, above 80 A of stirring current, crushed particles collided with each other and recombined.
(3) With regard to the effect of stirring time on microstructure, 60 s of stirring time resulted in the finest

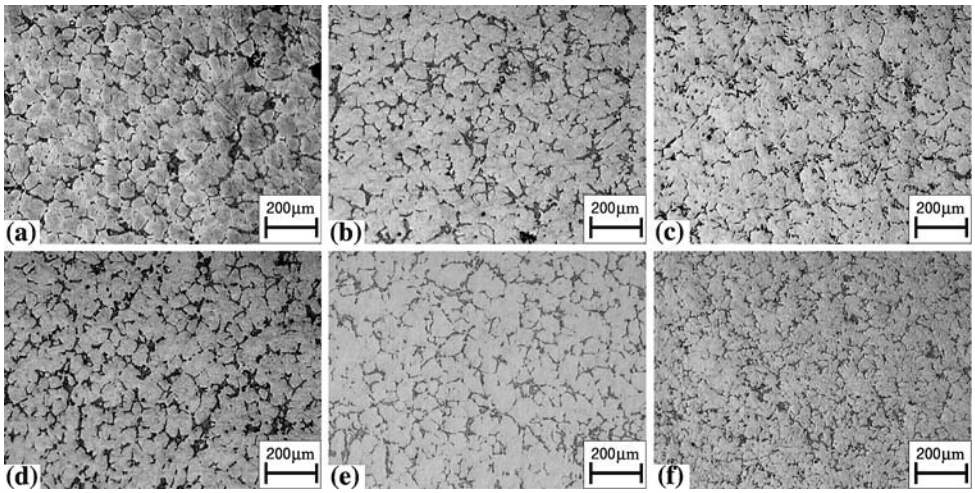

Fig. 11 The pictures of microstructure according to aging time for T6 in A6061; (a) without T6, (b) 2 h, (c) 4 h, (d) 6 h, (e) 8 h, (f) 12 h

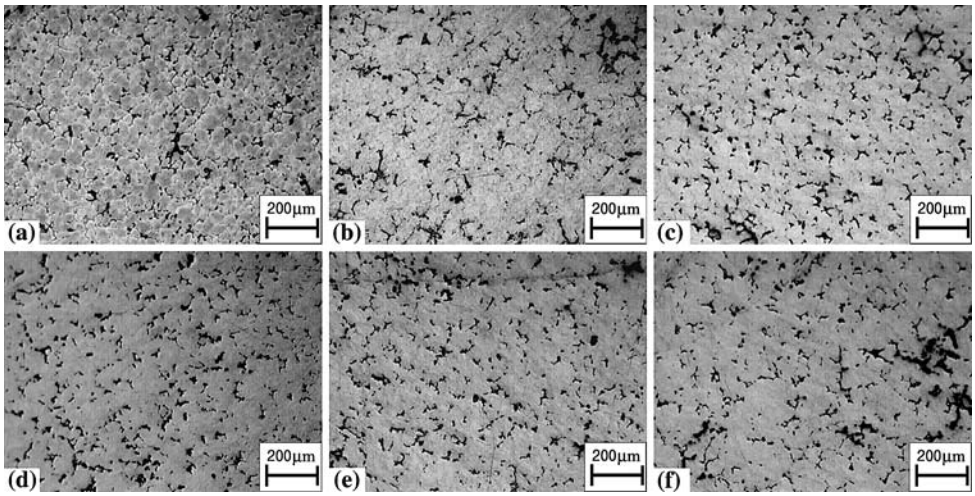

Fig. 12 The pictures of microstructure according to aging time for T6 in A7075; (a) without T6, (b) 4 h, (c) 8 h, (d) 12 h, (e) 24 h, (f) 36 h

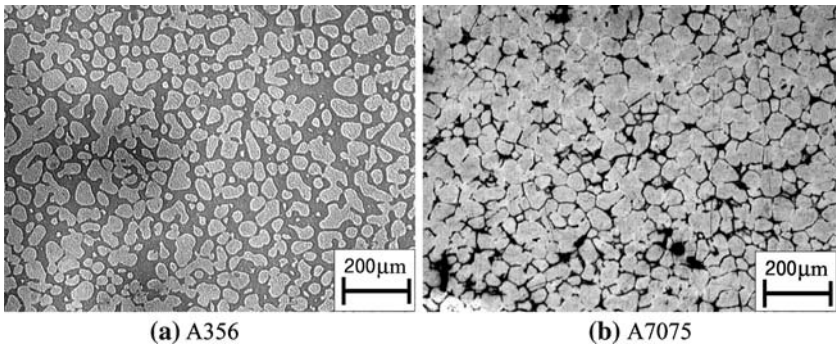

Fig. 13 Comparison of microstructure fabricated by EMS in A356 and A7075; (a) A356 (T_p: 655 °C, t_s: 60 s), (b) 7075 (T_p: 710 °C, t_s: 60 s)

and most globular structure for both A7075 and A6061 alloys.

(4) The temperature of the melts increased when measuring solidification speed of the melts using thermocouples during electromagnetic stirring of structural alloys.

(5) The optimal heat treatment conditions of A7075 and A6061 are solution treatment at 480 °C for 17 h and aging time at 120 °C for 24 h and solution treatment at 530 °C for 2 h and aging time at 177 °C for 4 h, respectively.

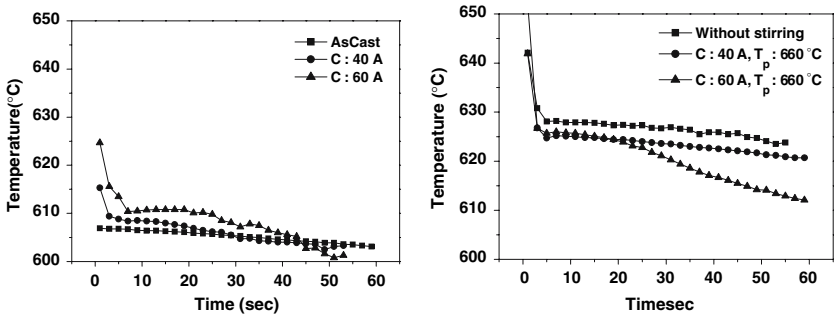

(a) A356, T_P = 650 °C **(b)** A7075, T_P = 660 °C

Fig. 14 Temperature variation curves according to each condition in A356 and A7075; (a) A356, T_p = 650 °C, (b) A7075, T_p = 660 °C

Acknowledgments

This work was supported by the Korea Science and Engineering Foundation (KOSEF) through the National Research Lab. Program funded by the Ministry of Science and Technology (No. R0A-2003-000-10435-0) and grants-in-aid for the National Core Research Center Program from MOST/KOSEF (No. R15-2006-022-02001-0).

References

1. S. Ji, Z. Fan, and M.J. Bevis, Semi-Solid Processing of Engineering Alloys by a Twin-Screw Rheomoulding Process, *Mater. Sci. Eng. A*, 2001, **299**, p 210–217
2. G. Chirmetta and L. Zanardi, Production of Structural Components by Thixoforming Aluminum Alloys, *Proc. of the 3rd Int. Conf. on Semi-Solid Processing of Alloys and Composites*, 1996 (Tokyo), p 235–244
3. M. Adachi, S. Sato, H. Sasaki, Y. Harasa, T. Maeda, and N. Ishibash, The Effect of Casting Condition for Mechanical Properties of Cast Alloys made with New Rheocasting Process, *Proc. of the 7th Int. Conf. on Semi-Solid Processing of Alloys and Composites*, 2002 (Tsukuba), p 629–634
4. C.G. Kang, P.K. Seo, and Y.P. Jeon, Thixo Diecasting Process for Fabrication of Thin-type Component with Wrought Aluminum Alloys and Its Formability Limitation, *J. Mat. Proc. Technol.*, 2005, **160**, p 59–69
5. M. Adachi and S. Sato, Advanced Rheocasting Process Improves Quality and Competitiveness. SAE 2000 World Congress, Michigan, 2000, p 21–37
6. C. Vives, Crystallization of Semi-solid Magnesium Alloys and Composites in the Presence of Magnetohydrodynamic Shear Flows, *J. Crystal Growth*, 1994, **137**, p 653–662
7. C. Vives, Elaboration of Metal Matrix Composites from Thixotropic Alloy Slurries Using a New Magnetohydrodynamic Caster, *Metall. Trans. B*, 1993, **24B**, p 493–510
8. D.H. No, S.M. Lee, and J.P. Hong, Solidification Characteristics of an Al-7wt%Si Alloy Produced by Pressurization in the Semi-Solid State After Stirring, *J. Korea Foundrymen's Soc.*, 1999, **19**, p 123–133
9. P. Kapranos and H.V. Atkinson, Thixoforming 2014, 6082, 7010 and 7075 aluminum wrought alloys, *Proc. of the 7th Int. Conf. on the Semi-Solid Processing of Alloys and Composites*, 2002 (Tsukuba), p 167–171
10. D. Liu, H.V. Atkinson, P. Kapranos, and H. Jones, Effect of Heat Treatment on Structure and Properties of Thixoformed Wrought Alloy 2014, *Proc. of the 7th Int. Conf. on the Semi-Solid Processing of Alloys and Composites*, 2002 (Tsukuba), p 311–316
11. S.C. Lim and E.P. Yoon, Refinement of Primary Crystals in Al Alloy by the Electromagnetic Stirring, *J. Korea Foundrymen's Soc.*, 1996, **16**, p 430–439